pH-metric study of the setting reaction of monocalcium phosphate monohydrate/calcium oxide-based cements

JOSIANE NURIT, JACQUES MARGERIT, ALAIN TEROL, PHILIPPE BOUDEVILLE*
Laboratoire de Chimie Générale et Minérale, Faculté de Pharmacie,
15 Avenue Charles Flahault, BP 14 491, 34093 Montpellier Cedex 5, France
E-mail: boudevil@pharma.univ-montp1.fr

Hydraulic calcium phosphate cements (CPCs) that are used as osseous substitutes, set by an acid–base reaction between an acid calcium phosphate and a basic calcium salt (often a phosphate). In order to gain a better understanding of the setting of the monocalcium phosphate monohydrate–calcium oxide cement that we developed and in the aim to improve its mechanical properties, the setting reaction was studied by pH-metry. The two methods described in the literature were used. In the first, cement samples were prepared then crushed after different storage periods at 37 °C, 100% RH. The powder was then immersed in pure water with stirring and the pH was measured after equilibration. In the second technique, the starting materials were poured into water while stirring and the pH were followed over time. The two methods gave different results. The first procedure provided information concerning the pH of the surrounding liquid following the partial dissolution of the cement components, rather than any information about pH changes during setting. The second method is more appropriate to follow the pH variations during setting. In this second procedure, the effects of different parameters such as crushing time, stirring rate, liquid-to-powder (L/P) ratio and temperature were investigated. These parameters may impact substantially on the shape and position of the $pH = f(t)$ curves. One or three pH jumps were observed during the setting depending on the composition of the liquid phase. The time at which these pH jumps occurred depended on the pH of the liquid phase, the concentration of the buffer, the crushing of starting materials, the L/P ratio and the temperature. Good linear correlations were obtained (i) between the time of the pH jumps and the L/P ratio and the temperature and (ii) between the time of the first pH jump and the compressive strength and the final setting time of the cements prepared with different liquid phases. It may be assumed in view of these correlations that the results obtained in dilute solution may be extrapolated to the conditions of cement sample preparation and that the mechanical properties of the cement are directly related to the phenomena that occur at the first pH jump which corresponds to precipitation of dicalcium phosphate dihydrate.

1. Introduction

Calcium phosphate cements (CPCs) are suitable for a number of applications in medicine and dentistry involving hard tissue replacement [1, 2]. Hydraulic CPCs set by an acid–base reaction between an acid calcium phosphate and a basic calcium salt (often a phosphate). Acid calcium phosphates can be monocalcium phosphate monohydrate (MCPM) or anhydrous (MCPA), dicalcium phosphate dihydrate (DCPD) or anhydrous (DCPA) or amorphous calcium phosphate (ACP). The basic calcium salts can be α or β tricalcium phosphate, (α or β-TCP), tetracalcium phosphate (TTCP), calcium oxide (CaO), calcium hydroxide ($Ca(OH)_2$) or calcium carbonate ($CaCO_3$). After mixing the powder with the liquid phase, the reactants dissolve in the liquid. This dissolution is followed by precipitation of a calcium phosphate that shows intermediate basicity, less soluble than the starting materials. It is the entanglement of the precipitated crystals that provides the cement cohesion and its mechanical strength. However, cement setting time depends on the rate at which supersaturation is reached, and this itself depends on the nature of the starting materials and their specific surface area. The solubility of calcium and phosphate salts depends on the pH of the liquid phase [3, 4]. Consequently, liquid phases of

*Author to whom all correspondence should be addressed.

TABLE I Experimental conditions in pH studies of the setting reactions of different calcium phosphate cements

Starting materials	Final product	L/P ratio(s) (ml g^{-1})	Time of measurement	Temperature (°C)	Ref.
DCPA/TTCP	HA	200, 100	7 days	25	26
DCPA/TTCP	HA	5	12 h	38	27
MCPM/$Ca(OH)_2$/TTCP	CDHA	100, 1	24 h, 15 min	25	28
DCPD/TTCP/$MgCl_2$	CDHA	5	35 h	37.4	29
DCPD/TTCP	HA or CDHA	5	12 h, 6 months	25, 37.4, 50	25
DCPA/TTCP	HA	2.5	14 h	25, 37.4	24
DCPA/TTCP	HA	0.5	4 h	25	23
β-TCP/MCPM or H_3PO_4	DCPD	10	80 min	25	10
α-TCP/DCPA	HA	35	9 h	25	30

different pH values such as orthophosphoric acid [4–7], pure water [6, 8–10] and buffers composed of sodium, potassium or ammonium phosphate [11, 12] or others [13–15] are used to prepare the different CPCs developed. The use of a phosphate buffer logically shortens the setting time of apatitic cements [11, 16–18] because the solubility of stoichiometric hydroxyapatite (HA) or calcium deficient hydroxyapatite (CDHA) is minimum at neutral pH. The effect of phosphate buffers on compressive strength (CS) is more ambiguous: Ishikawa *et al*. [11] did not observe any difference for a cement made of DCPA and TTCP; Fernandez *et al*. [18] obtained a decrease in the CS of α-TCP or DCPA and α-TCP-based cements, while we noted a substantial increase in the CS of the MCPM–CaO cement we developed [19–20]. To understand the origin of this paradoxical behavior and optimize the formulation of our cement, we carried out the pH-metric study of the setting reaction of this cement.

Two methods are described in the literature to study the pH changes of a cement during its setting. In the first [21, 22] cement samples are prepared then crushed after different storage periods at 37 °C, 100% RH. The powder is then immersed in pure water, while stirring, at a liquid-to-powder ratio of 200 ml g^{-1} and the pH is measured after equilibration (Ginebra MP, personal communication). In the second technique [23–30], the starting materials are poured into water, while stirring, and the pH is followed over time. However, experimental conditions reported such as the liquid-to-powder ratio (L/P), the temperature and the measurement duration vary considerably from one experiment to another (Table I) and the results obtained in such conditions are therefore difficult to extrapolate to the conditions of cement preparation. Consequently, we also investigated the effect of some parameters on the pH vs. time plots.

2. Materials and methods

2.1. Chemicals and materials

All chemicals were of analytical grade obtained from Aldrich (CaO), Fluka (MCPM, NaH_2PO_4, $Na_2HPO_4 \cdot 12(H_2O)$, $Ca(OH)_2$) or Prolabo (H_3PO_4). Commercial CaO was heated at 900 °C for 2 h to remove H_2O and CO_2 and stored in a vacuum desiccator. The CaO particle size was around 7 μm (d_{10}–d_{90}: 2–40 μm; specific area: 1.3 m^2 g^{-1}, Mastersizer, Malvern Instruments). Commercial MCPM contained 3% moisture (determined by thermogravimetry) and 5% free H_3PO_4 (determined by acidimetry); particle size was around 230 μm (50–700; specific area: 0.06 m^2 g^{-1}). The commercial powder was ground for 5 h in a rotating micromill (Retsch Instruments) before use to obtain a final particle size of around 20 μm (5–130; specific area: 0.60 m^2 g^{-1}) and was used without further processing. Water was double distilled on quartz after deionization on an ion-exchange resin and rendered CO_2-free by boiling.

The potentiometric study was performed on a WTW pH-meter using a combined WTW Sentix 96 (pH 0.5–13; 0–80 °C) glass electrode fitted with a Pt probe for temperature correction and calibrated using two NBS buffers (pH 7 and 4, Fluka buffer standard solution color-coded). Powder X-ray diffraction (XRD) patterns were obtained with an automatic Philips Diffractometer controlled by an IBM PC (5 or 36 acquisitions, 2–20°θ, 900 points, acquisition delay 500 ms) using a Cu anti-cathode ($K_{\alpha 1} = 0.15405$ nm) with a nickel filter. Differential scanning calorimetry (DSC) was performed using a DSC4 Perkin-Elmer computer-managed calorimeter. Indium was used as the calorimetric and thermometric reference. All experiments were performed under nitrogen flow, on 2–3 mg samples in closed aluminum pellets. The heating rate was 20 °C min^{-1}.

2.2. Preparation of the cement samples

Cement powder was prepared by weighing the two components (MCPM and CaO) in the stoichiometric ratio given in Equation 1 and mixing just before use by manual crushing for 30 s in an agate mortar.

$$3Ca(H_2PO_4)_2 \cdot H_2O + 7CaO \rightarrow Ca_{10}(PO_4)_6(OH)_2 + 8H_2O \quad (1)$$

The liquid phase was either pure water or 1 M H_3PO_4 or 0.25 M, 0.45 M, 0.75 M or 1 M sodium phosphate (NaP) buffers, pH 4, 7 or 9 prepared from NaH_2PO_4 and $Na_2HPO_4 \cdot 12(H_2O)$. The liquid-to-powder (L/P) ratio was 0.55 ml g^{-1}. It is noteworthy that when the liquid phase contained phosphate, the amount of phosphate was taken into account to obtain a final calcium-to-phosphate ratio of 1.67 in the cement. The powder was incorporated into the liquid by successive fractions in the same manner as for dental zinc phosphate cements (1/6 of the powder was added every 15 s) and kneaded with a spatula

between each addition to produce a paste of workable consistency. After mixing for a total of 2 min on a glass plate at 20 ± 1 °C, the paste was loaded into the molds and stored at 37 °C, 100% RH.

2.3. pH measurement procedures

Both methods described in the literature were used. In the first, cement samples stored at 37 °C were removed from their molds at different periods then crushed and 125 mg of the resulting powder was transferred into 25 ml of CO_2-free water thermostated at 25 °C (L/P = 200 ml g^{-1}), while stirring. The pH of the suspension was then followed until it stabilized.

In the second procedure, aliquot parts of the starting materials (powder and liquid phase corresponding to cements with Ca/P = 1.67 and L/P = 0.55 ml g^{-1}) were poured in CO_2-free water to obtain a final volume of 10 ml and different final liquid-to-powder ratios ranged from 2 to 15 ml g^{-1}. As an example to obtain a final L/P ratio of 5, 2 g of the MCPM–CaO mixture was added to a 20-ml flask containing 1.1 ml of buffer and 8.9 ml of water. The flask was immersed in a bath at 25, 37 or 50 °C. The suspension was stirred on a magnetic stirrer. The pH of the medium was recorded for up to 7.5 h. The effect of certain parameters such as powder crushing, stirring rate, L/P ratio and temperature on the pH = $f(t)$ plot profile was investigated. For clarity, certain specific experimental conditions are described and discussed in the result section because their choice was the consequence of previous experiments.

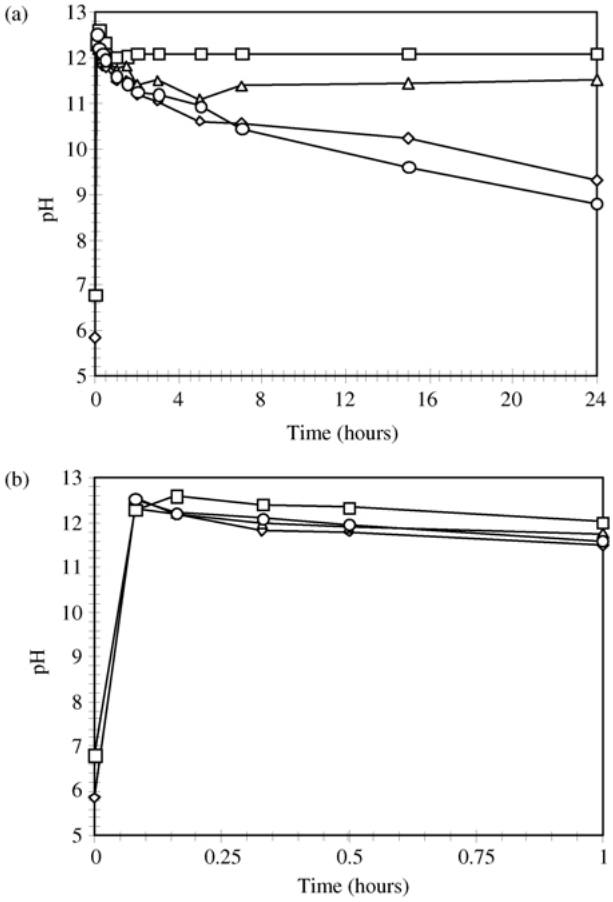

Figure 1 Variation in the pH of the suspension obtained by dispersion of crushed cement samples as a function of the time of crushing after mixing and storage at 37 °C, 100% RH (first procedure) and prepared with different liquid phases: (○) 1 M H_3PO_4; (◇) H_2O; (□) 0,45 M pH 7 ; (△) 1 M pH 7 NaP buffer. L/P ratio = 200 ml g^{-1}. (a) up to 24 h, (b) during the first hour.

3. Results

3.1. pH = $f(t)$ plots obtained with the first procedure

The pH = $f(t)$ plots obtained using the first procedure where cement samples were prepared with 1 M H_3PO_4, H_2O, 0.45 or 1 M pH 7 NaP buffer as liquid phase are presented in Fig. 1. Here, the pH for all the samples rose to a value of 12.5 and the plots were similar over the first hour (Fig. 1(b)). Thereafter, the pH value stabilized at around 11.5–12 when a pH 7 NaP buffer was used as liquid phase, while it decreased toward neutrality with water or 1 M H_3PO_4 (Fig. 1(a)). These two different behaviors are consistent with the mechanism proposed subsequent to the XRD and DSC studies of the setting reaction [19]. Indeed, it was shown that the setting reaction proceeded in two steps: (i) rapid formation of DCPD by reaction of MCPM with part of the CaO, Equations 2 and 3, then (ii) a slower reaction of the newly formed DCPD with the remaining CaO. When water or orthophosphoric acid solutions were used as the liquid phase, this second produced stoichiometric hydroxyapatite in less than 24 h, Equation 4, and this explains the pH value decrease toward neutrality, while with NaP buffers, 30% of the DCPD remained after 3 days and the final composition of the cement, even after 3 months, was a mixture of calcium-deficient hydroxyapatite and calcium hydroxide [31], Equation 5.

$$3Ca(H_2PO_4)_2 \cdot H_2O + 3CaO + 6H_2O \rightarrow 6CaHPO_4 \cdot 2(H_2O) \quad (2)$$

$$(3 - x/2)Ca(H_2PO_4)_2 \cdot H_2O + 3CaO + xNaP + 6H_2O \rightarrow 6CaHPO_4 \cdot 2(H_2O) + yNa^+ \quad (3)$$

$$6CaHPO_4 \cdot 2(H_2O) + 4CaO \rightarrow Ca_{10}(PO_4)_6(OH)_2 + 14H_2O \quad (4)$$

$$6CaHPO_4 \cdot 2(H_2O) + 4CaO + yNa^+ \rightarrow CDHA + wCa(OH)_2 + zH_2O \quad (5)$$

The CDHA contained Na^+ ions drawn from the NaP buffer but the replacement of one Ca^{2+} by two Na^+ was not systematic because, after three months, the amount of calcium hydroxide appeared to be independent of the NaP buffer concentration [31]. The presence of $Ca(OH)_2$ was responsible for the high pH value observed over 24 h following the cement dissolution and for the antimicrobial potency of this cement [32].

3.2. pH = $f(t)$ plots obtained with the second procedure

The pH = $f(t)$ plots recorded using the second procedure where cements were prepared with 1 M H_3PO_4, H_2O, 0.45 or 1 M pH 7 NaP, 1 M pH 4 NaP or 1 M pH 9 NaP buffer as liquid phase are presented in Fig. 2. Two different plot shapes were again observed. When NaP

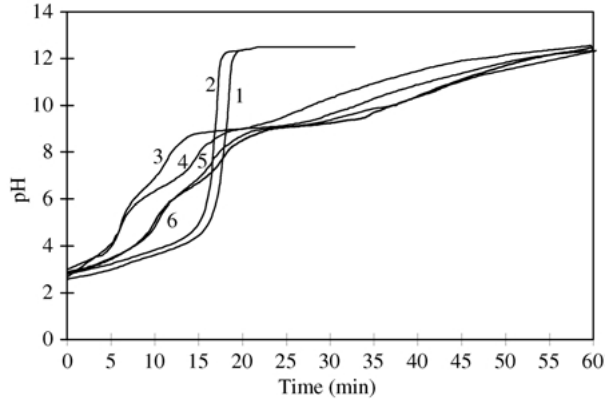

Figure 2 Variation in the pH of the suspension obtained by dispersion of starting materials as a function of the time (second procedure). Powder: 2 g of MCPM + CaO mixture (Ca/P = 1,67) crushed 30 s; liquid phase: 8.9 ml of water + 1.1 ml of (1) 1 M H_3PO_4, (2) H_2O, (3) 1 M pH 7, (4) 1 M pH 9, (5) 0.45 M pH 7 and (6) 1 M pH 4 NaP. Final L/P ratio = 5 ml g^{-1}, $\theta = 25\,^{\circ}C$.

buffer was not included in the liquid phase (H_3PO_4, H_2O), the $pH = f(t)$ plot showed only a single pH jump whereas all preparations with NaP buffer showed three pH jumps. The time points corresponding to the jumps, determined from the maximums of the derived curve $d(pH)/dt = f(t)$, were labeled $t_{1\,max}$, $t_{2\,max}$ and $t_{3\,max}$ respectively. These times were reproducible and correlated with the compressive strength (CS) and final setting time (F) of the cement samples prepared with the different liquid phases [19]. A good linear correlation was obtained between CS and $t_{1\,max}$ $(CS = (34.7 - 1.72\ t_{1\,max})$ MPa, $r = 0.984$, Fig. 3, and between F and $t_{1\,max}$, $F = (3.5 + 0.48\ t_{1\,max})$ min, $r = 0.991$ if we except the value obtained for 1 M H_3PO_4). This shows that the mechanical properties of the cement are certainly dependent on phenomena occurring at the first pH jump. However, to be sure that these correlations obtained under experimental conditions (L/P = 5 ml g^{-1}, $\theta = 25\,^{\circ}C$ and stirred suspension) that differ from those used to prepare cement samples (L/P = 0.55 ml g^{-1}, $\theta = 37\,^{\circ}C$ and unstirred suspension), we investigated the impact of these parameters on the $pH = f(t)$ plot profile.

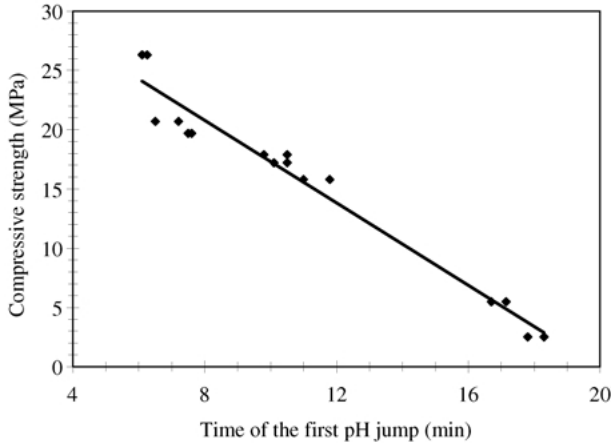

Figure 3 Correlation between the compressive strength of cement samples prepared with different liquid phases and the time of occurrence of the first pH jump $t_{1\,max}$.

3.3. Effect of the crushing of the starting material mixture

To obtain a homogeneous powder, the two solid starting materials, MCPM and CaO, were manually crushed in an agate mortar for 30 s. But, the same experiments performed by different operators resulted in $pH = f(t)$ plot of different shapes and positions. This was due to the fact that the different operators applied different crushing strengths. A new crushing procedure was therefore adopted. Because commercial MCPM contains free H_3PO_4 and moisture, the powder is sticky and lumpy, even after mechanical grinding to reduce particle size. Thus, MCPM was first manually crushed in an agate mortar for 20 s to break up the lumps and CaO was added. The preparation was then mixed with MCPM for 15 s using a spatula. Finally, the mixture was vigorously crushed, always by the same operator, for different periods of up to 90 s. Changes in the shape and position of the $pH = f(t)$ curve were plotted against crushing time and are presented in Fig. 4. By increasing crushing time up to 60 s, the two first pH jumps occurred more rapidly, then $t_{1\,max}$ and $t_{2\,max}$ stabilized. The third part of the plot was considerably changed since the pH jump was transformed into a pH drop followed by a slow but continuous pH increase. Since the shape and position of the curve did not change significantly after 60 s of crushing, this crushing time was retained for the subsequent experiments.

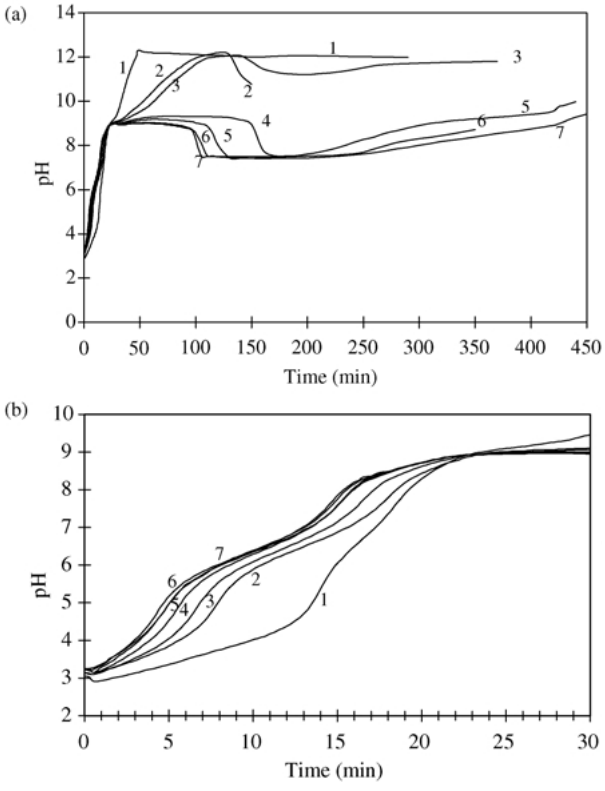

Figure 4 Variation in the $pH = f(t)$ curve shape and position with the crushing time of the mixture MCPM–CaO: (1) = 0 s, (2) = 15 s, (3) = 30 s, (4) = 45 s, (5) = 60 s, (6) = 75 s, (7) = 90 s. Ca/P = 1.67, 1 M pH 7 NaP buffer; L/P = 5; stirring = 5 and $\theta = 25\,^{\circ}C$. (a) during 7.5 h, (b) during the first 30 min.

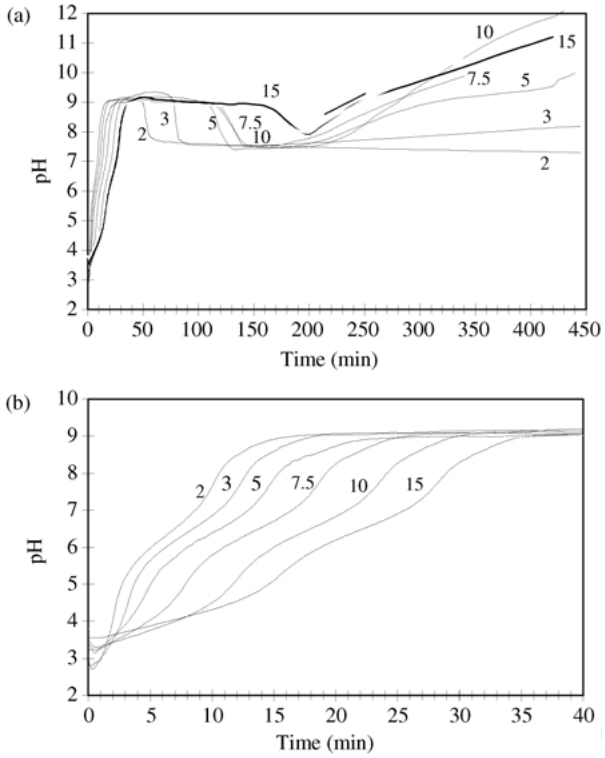

Figure 5 Variation in the pH = $f(t)$ curve shape and position as a function of the L/P ratio (indicated on each curve) ; Ca/P = 1.67; 1 M pH 7 NaP buffer; crushing time 60 s; stirring = 5; θ = 25 °C. (a) during 7.5 h, (b) during the first 40 min.

3.4. Effect of stirring rate

The liquid phase was stirred on a magnetic stirrer to maintain the powder in suspension. Since stirring rate may affect reactant dissolution rate and subsequent product precipitation, this parameter was also tested. No effect was noted on $t_{1\,max}$ and $t_{2\,max}$; only $t_{3\,max}$ was very slightly affected. A stirring rate corresponding to the graduation 5 of the magnetic stirrer, already used for the previous experiments, was retained.

3.5. Effect of liquid-to-powder ratio

This parameter was varied from 15 to 2 to approach as closely as possible the conditions of cement preparation. The changes in the pH = $f(t)$ plots are presented in Fig. 5. Only the position of the two first pH jumps changed when the L/P ratio was decreased (Fig. 5(b)). In the third part of the plot, the pH drop occurred sooner and the subsequent rise in the pH was slower and lower. It is noteworthy that when the L/P ratio corresponded to 2, the cement set after 1 h. This could explain the lack of any variation in the pH observed. Indeed, the same invariance in the pH value was observed by Liu *et al*. [23] after their slurries set hard. For the other L/P ratios, the suspension converted more or less rapidly into a gel that remained stable for several days. $t_{1\,max}$, $t_{2\,max}$ and $t_{3\,max}$ were plotted against the L/P ratio (Fig. 6). $t_{1\,max}$ and $t_{2\,max}$ were directly related to the L/P ratio value, Equations 6 and 7, but the relation for the pH drop ($t_{3\,max}$) was not linear (Fig. 6).

$$t_{1\,max} = 1.02\ \text{L/P} + 0.0308 \quad r = 0.999 \qquad (6)$$

$$t_{2\,max} = 1.36\ \text{L/P} + 7.98 \quad r = 0.998 \qquad (7)$$

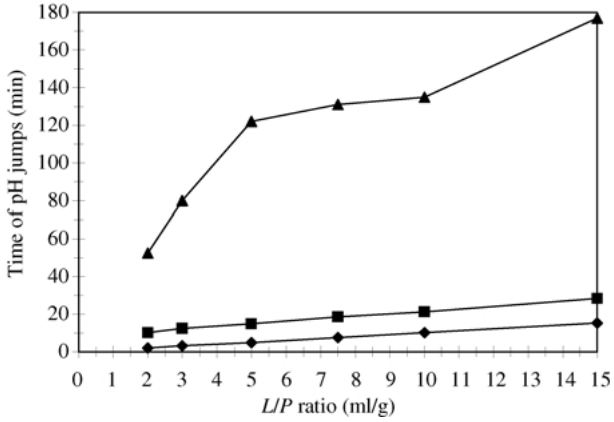

Figure 6 Variations in $t_{1\,max}$ (◆), $t_{2\,max}$ (■) and $t_{3\,max}$ (▲) with the L/P ratio. Ca/P = 1.67; NaP buffer pH 7, 1 M ; crushing time 60 s; stirring = 5 and θ = 25 °C.

3.6. Effect of temperature

The pH was plotted over time at 25, 37 and 50 °C for a slurry with L/P = 5 ml g^{-1} (Fig. 7). The higher the temperature, the faster the reaction was. The drop in the pH value was both more rapid and more substantial because of the retrograde solubility of the DCPD and $Ca(OH)_2$. The $t_{1\,max}$ and $t_{2\,max}$ periods correlated with the temperature, Equations 8 and 9.

$$t_{1\,max} = (-0.12\theta + 7.82)\ \text{min} \quad r = 0.997 \qquad (8)$$

$$t_{2\,max} = (-0.29\theta + 21.7)\ \text{min} \quad r = 0.985 \qquad (9)$$

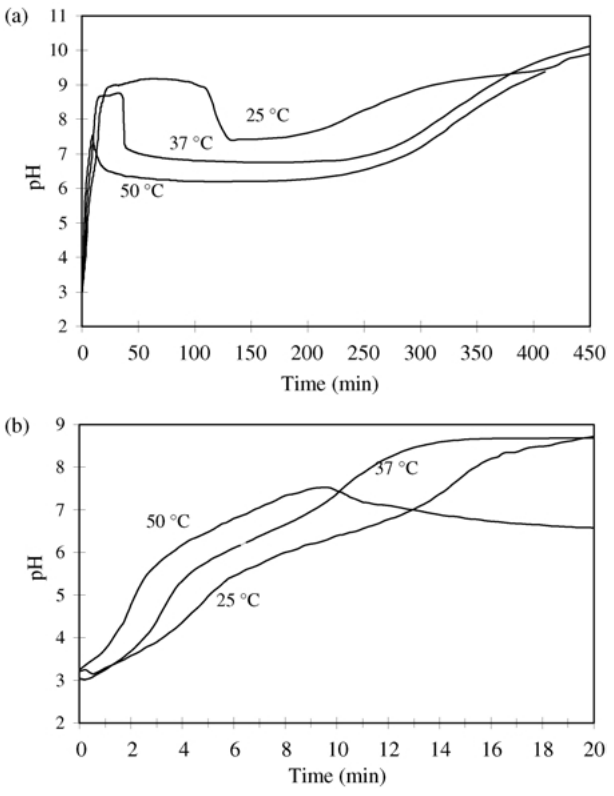

Figure 7 Variation in the pH = $f(t)$ curve shape and position as a function of the temperature (indicated on each curve). Ca/P = 1.67 crushing time = 60 s; 1 M pH 7 NaP buffer; L/P = 5; stirring = 5. (a) during 7.5 h, (b) during the first 20 min.

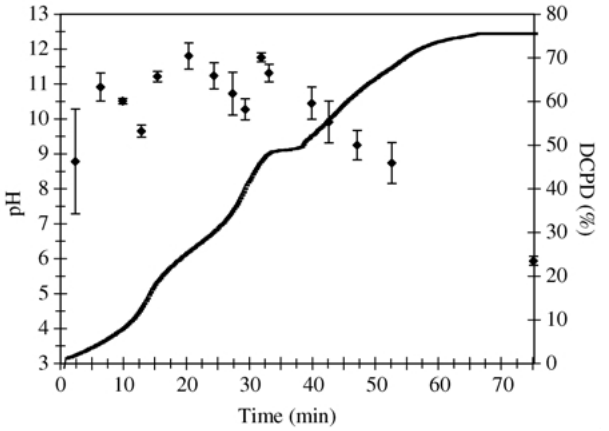

Figure 8 Variation in the pH of the suspension (full line) and in the percentage of DCPD present (◆) in the solid phase with time. Ca/P = 1.67; 1 M pH 7 NaP buffer and L/P = 5; stirring = 5; θ = 25 °C; 10 g of 60-s crushed powder.

3.7. Changes in the composition of the solid phase over time

Powder (10 g) corresponding to Ca/P = 1.67 was poured rapidly into a 100-ml glass flask immersed in a thermostated bath at 25 °C and containing 50 ml of liquid phase (5.5 ml of 1 M pH 7 NaP buffer + 44.5 ml of CO_2 free water) while stirring (global L/P ratio of 5).The pH was measured continuously. Then, at different intervals corresponding to specific pH values (beginning, middle and end of the different pH jumps), 2 ml of the suspension were removed and rapidly filtered into a fritted glass filtering flask (porosity 4) under vacuum. Because the reaction rate increases as the L/P ratio is lowered, the solid phase was washed directly on the filter with ethanol to stop the reaction. The solid residue was then quenched in liquid nitrogen and freeze-dried. The freeze-dried samples were analyzed by XRD to identify the different components of the solid phase and by DSC to quantify the DCPD mass percentage at any given moment. The changes in pH and in the percentage of DCPD over time are presented in Fig. 8. This figure shows that the two first pH jumps correspond to a significant reduction in the DCPD percentage of the solid phase. Complete conversion of MCPM to DCPD, Equations 2 or 3, would lead theoretically to 82% (w/w) DCPD in the dry solid phase. Because non negligible amounts of calcium and phosphate are dissolved in the liquid phase, the maximum DCPD values of 72% reached after 21 and 32 min would indicate that phosphate groups in the solid phase were essentially present as DCPD. XRD analyses showed that MCPM had completely disappeared after 2 min to give DCPD. An amorphous-like background appeared then disappeared twice, and finally remained present. This amorphous-like background appeared to be maximal when the DCPD percentage was lowest and vice versa. Finally, CaO decreased rapidly overe the first 15 min, then more slowly without any concomitant appearance of $Ca(OH)_2$. No CaO remained after 75 min and CDHA began to precipitate.

4. Discussion

The two pH measurement methods gave different results, as shown by Figs. 1 and 2. The first procedure provided information about the pH of the surrounding liquid following the partial dissolution of cement components rather than information on the pH changes during setting. Because CaO and $Ca(OH)_2$ are more soluble than DCPD, the pH is logically basic. The second method is more appropriate to follow pH variations during setting.

In this second procedure, parameters such as crushing time, L/P ratio and temperature may substantially affect the shape and position of the plots (Figs. 4–7). But, once the powder crushing procedure was standardized to obtain reproducible results, excellent correlations were obtained between the times corresponding to the pH jumps ($t_{1\,max}$ and $t_{2\,max}$) or drop ($t_{3\,max}$) and the parameters such as L/P ratio and temperature. Using a NaP buffer as liquid phase, the changes in the $pH = f(t)$ plots with the L/P ratio and with the temperature indicate that the three steps observed at high L/P ratios (L/P = 5 or 10 for example) also occur under the conditions employed for cement preparation (L/P = 0.55). The model is transposable and the linear regressions allow the results obtained under dilute conditions to be extrapolated to the preparation conditions of cement samples. At 25 °C and an L/P ratio of 0.55 ml g^{-1}, Equation 6 gives $t_{1\,max} = 0.6$ min and Equation 7 gives $t_{2\,max} = 8.7$ min. The first pH jump occurs before 2 min, i.e. during kneading with the spatula on the glass plate. The second jump appears when the cement hardens. The extrapolation of $t_{3\,max}$ at 25 °C from the three first points of the $t_{3\,max} = f(L/P)$ plot (Fig. 6) gives a time of 21 min for its occurrence, but since the cement is stored at 37 °C and since the temperature shortens the appearance of $t_{3\,max}$, it is very likely reached around 15 min.

The decrease in $t_{1\,max}$, $t_{2\,max}$ and $t_{3\,max}$ when the L/P ratio falls is logical because the oversaturation is reached more rapidly in smaller volume of liquid and the DCPD precipitates sooner, consuming first MCPM, and consequently the pH rises more rapidly. Although the reactor was immersed in a thermostated bath, the heat dissipated by the reaction responsible for the first pH jump and the hydrolysis of CaO can heat the solution, and all the more so when a small volume of liquid is involved. Because of the retrograde solubility of DCPD, $Ca(OH)_2$ and CDHA, an increase in the temperature of the medium leads to their precipitation and the precipitation of $Ca(OH)_2$ may be responsible for the pH drop that occurs all the more rapidly that the L/P ratio is low (Fig. 5). This suggestion is reinforced by the variations observed in the $pH = f(t)$ plots by increasing the temperature of the thermostated bath (Fig. 7). In the course of these heating experiments the pH jumps and the pH drop occurred sooner and the pH drop was more substantial. But this explanation should be verified by following both the pH and the temperature of the slurry in an adiabatic calorimeter as performed by Brown *et al*. [33]. Theses experiments are planned.

The effect of powder crushing time on the position and shape of the $pH = f(t)$ plots (Fig. 4) might be explained as follows. Because commercial MCPM is not pure, it contains moisture and free orthophosphoric acid, the powder is therefore sticky and shares lumps. By grinding the MCPM powder with CaO in the mortar, the orthophosphoric acid reacts with CaO to give an equivalent amount of DCPD and/or DCPA, and the

moisture partly hydrates CaO to form $Ca(OH)_2$. The formation of these three products in low amounts was highlighted by XRD [20]. During the crushing operation, the aggregates were broken up, the H_3PO_4 and water disappeared and the powder became fluid with an increase in its specific surface area [20]. Since the powder presents a greater specific surface area, its dissolution is faster, the oversaturation is reached more rapidly and DCPD precipitation and $t_{1\,max}$ will occur sooner. Moreover, the DCPD, present in a small amount in the crushed powder, could serve as centers of nucleation to favor the subsequent precipitation of DCPD for which the formation is kinetically favored at low pH [28]. The changes in the $pH = f(t)$ plots with crushing time (Fig. 4) suggests that this pseudo-solid state reaction during manual crushing was achieved after 1 min because the shape and position of the $pH = f(t)$ plot did not change significantly after this time.

The results obtained by XRD analysis of powder composition over time (Fig. 8) confirm some of the observations deduced from the kinetic study of the setting reaction [19], Equations 2–5: MCPM is rapidly converted into DCPD that then reacts with the remaining CaO. The amorphous-like background observed intermittently on the XRD patterns suggests the presence of a non-crystalline calcium phosphate (NCP) with a Ca/P ratio between 1.2 and 1.35 [25]. NCP, also called ACP has been shown to be an intermediate product in a number of studies on HA or bone formation [34]. The appearance of a NCP during a cement setting reaction was also noted by Tenhuisen and Brown [25, 29, 34] in their studies on the DCPD (or DCPA)–TTCP system which is similar to our system once MCPM has been converted to DCPD.

The shape of the $pH = f(t)$ plot (Fig. 8) is very similar to the titration curve of H_3PO_4 by a strong base. Despite the presence of the pH 7 NaP buffer in the liquid phase, the pH at the beginning of the curve is low (around 3). The incongruent dissolution of MCPM [35], resulting in the formation of brushite and H_3PO_4, may explain this low pH value. The concomitant dissolution and hydrolysis of CaO result in calcium and hydroxyl ions that may react as shown in the following possible equations:

$$H_3PO_4 + OH^- \rightarrow H_2PO_4^- \quad (10)$$

$$CaHPO_4\downarrow + uCa^{2+} \rightarrow NCP\downarrow (0.2 < u < 0.35) \quad (11)$$

$$NCP\downarrow + vH_2PO_4^- \rightarrow wCaHPO_4\downarrow + vH^+ \quad (12)$$

$$NCP\downarrow + xCa(OH)_2 + yNa^+ \rightarrow CDHA\downarrow + zOH^- \quad (13)$$

$$H_2PO_4^- + OH^- \rightarrow HPO_4^{2-} + H_2O \quad (14)$$

By combining these reactions, an attempt could be made to explain the pH jumps and the relative variations in the percentages of DCPD, NCP and/or CDHA in the solid phase. But, because the relative mass of this solid phase in comparison with the liquid phase volume and the time-course changes in the concentration of the different species in the liquid phase were not determined in this study, any explanation would be unreasonable without these data. These experiments are planned to gain a better understanding of the setting reaction of the cement we have developed and particularly to investigate the ambiguous role played by the sodium ions.

5. Conclusion

The first conclusion of this work is that the second pH measurement procedure is the most suitable to follow changes in pH during cement setting and it was therefore the most used (Table I). But, to be sure that the results are representative of the reactions that take place during cement setting, experiments have to be performed under experimental conditions as close as possible to cement preparation conditions. Indeed, if only the results obtained at $L/P = 5$ and above are considered with a short crushing time for the starting reactant mixture, it would be concluded that the pH of the cement during its setting rapidly becomes very alkaline. In fact, it remains close to neutrality during its setting and the alkalinity is only expressed in the course of its partial dissolution.

The changes in the $pH = f(t)$ plot with the different parameters indicate that, for the MCPM/CaO-based cement, the results obtained in dilute suspension are transposable to cement preparation conditions. This possible transposition validates the correlations between CS or final setting time and the time at which the first pH jump $t_{1\,max}$ occurs with an L/P ratio of $5\,ml\,g^{-1}$. The mechanical properties of this cement are in direct relation with the phenomena that occur during this first pH jump, principally the DCPD precipitation. Each parameter that will facilitate the DCPD precipitation will increase the CS and decrease the final setting time, and vice versa. However, further experiments are required to gain a full understanding of the MCPM/CaO-based cement setting reaction and identify the role played by the sodium ions.

Acknowledgment

The authors wish to thank B. Pauvert for his technical assistance.

References

1. K. ISHIKAWA, Y. MIYAMOTO, M. NAGAMAYA and K. ASAOKA, *Biomaterials* **16** (1995) 527 and ref. 1–11 therein.
2. F. C. M. DRIESSENS, M. G. BOLTONG, M. I. ZAPATERO, R. M. H. VERBEECK, W. BONFIELD, O. BERMUDEZ, E. FERNANDEZ, M. P. GINEBRA and J. A. PLANELL, *J. Mater. Sci. Mater. Med.* **6** (1995) 272 and refs 3–35 therein.
3. F. C. M. DRIESSENS, in ''Bioceramics of Calcium Phosphate'', edited by K. de Groot (CRC Press, Boca Raton, Florida, 1983).
4. W. E. BROWN and L. C. CHOW. Dental restorative cement pastes. US Patent 4 518 430 (1985).
5. J. L. LACOUT, E. MEJDOUBI and M. HAMAD, *J. Mater. Sci. Mater. Med.* **7** (1996) 371.
6. I. C. ISON, M. T. FULMER, B. M. BARR and B. R. CONSTANTZ, in ''Hydroxyapatite and Related Materials'' edited by P. W. Brown and B. R. Constantz (CRC Press and London, 1994) p. 215.
7. P. FRAYSSINET, L. GINESTE, P. COMTE, J. FAGES and N. ROUQUET, *Biomaterials* **19** (1998) 971.
8. O. BERMUDEZ, M. G. BOLTONG, F. C. M. DRIESSENS and J. A. PLANELL, *J. Mater. Sci. Mater. Med.* **4** (1993) 389.
9. F. C. M. DRIESSENS, M. G. BOLTONG, O. BERMUDEZ and J. A. PLANELL, *ibid.* **4** (1993) 503.
10. M. BOHNER, P. VAN LANDUYT, H. P. MERKLE and J. LEMAITRE, *ibid.* **8** (1997) 675.

11. K. ISHIKAWA, S. TAKAGI, L. C. CHOW and Y. ISHIKAWA, *ibid.* **6** (1995) 528.
12. M. P. GINEBRA, E. FERNANDEZ, M. G. BOLTONG, O. BERMUDEZ and J. A. PLANELL, F. C. M. DRIESSENS, *Clin. Mater.* **17** (1994) 99.
13. K. KURASHINA, H. KURITA, M. HIRANO, J. M. A. DE BLIECK, C. P. A. T. KLEIN and K. DE GROOT, *J. Mater. Sci. Mater. Med.* **6** (1995) 340.
14. T. KOSHINO, W. KUBOTA and T. MORII, *Biomaterials* **16** (1995) 125.
15. D. KNAACK, M. GOAD, M. AILOVA, C. REY, A. TOFIGHI, P. CHAKRAVARTHY and D. DUKE LEE, *J. Biomed. Mater. Res. (Appl Biomater)* **43** (1998) 399.
16. F. C. M. DRIESSENS, M. G. BOLTONG, J. A. PLANELL, O. BERMUDEZ, M. P. GINEBRA and E. FERNANDEZ, *Bioceramics*, vol. 6, edited by P. Ducheyne and D. Christiansen (Proceedings of the 6th International Symposium on Ceramics in Medicine, Philadelphia, USA, November 1993) (Butterworth-Heinemann, 1993) p. 469.
17. L. C. CHOW, S. TAKAGI and K. ISHIKAWA, in ''Formation of Hydroxyapatite in Cement Systems. Hydroxyapatite and Related Materials'', edited by P. W. Brown and B. Constantz (CRC Press, London, 1994) p. 127.
18. E. FERNANDEZ, M. G. BOLTONG, M. P. GINEBRA, O. BERMUDEZ, F. C. M. DRIESSENS and J. A. PLANELL, *Clin. Mater.* **16** (1994) 99.
19. P. BOUDEVILLE, S. SERRAJ, J. M. LELOUP, J. MARGERIT, B. PAUVERT and A. TEROL, *J. Mater. Sci. Mater. Med.* **10** (1999) 99.
20. S. SERRAJ, P. BOUDEVILLE and A. TEROL, *ibid.* **12** (2001) 45.
21. F. C. M. DRIESSENS, M. G. BOLTONG, O. BERMUDEZ, J. A. PLANELL, M. P. GINEBRA and E. FERNANDEZ, *ibid.* **5** (1994) 164.
22. O. BERMUDEZ, M. G. BOLTONG, F. C. M. DRIESSENS and J. A. PLANELL, *ibid.* **5** (1994) 160.
23. C. LIU, W. SHEN, Y. GU and L. HU, *J. Biomed. Mater. Res.* **35** 1 (1997) 75.
24. R. I. MARTIN and P. W. BROWN, *ibid.* **35**(3) (1997) 299.
25. K. S. TENHUISEN and P. W. BROWN, *ibid.* **36**(2) (1997) 233.
26. P. W. BROWN, N. HOCKER and S. HOYLE, *J. Am. Ceram. Soc.* **74**(8) (1991) 1848.
27. R. I. MARTIN and P. W. BROWN, *J. Mater. Sci. Mater. Med.* **5** (1994) 96.
28. M. T. FULMER, R. I. MARTIN and P. W. BROWN, *ibid.* **3** (1992) 299.
29. K. S. TENHUISEN and P. W. BROWN, *J Biomed. Mater. Res.* **36**(3) (1997) 306.
30. E. FERNANDEZ, F. J. GIL, M. P. GINEBRA, F. C. M. DRIESSENS, J. A. PLANELL and S. M. BEST, *J. Mater. Sci. Mater. Med.* **10** (1999) 223.
31. S. SERRAJ, P. MICHAÏLESCO, J. MARGERIT, B. BERNARD and P. BOUDEVILLE, *ibid.* **13** (2002) 125–131.
32. M. KOUASSI, P. MICHAÏLESCO and P. BOUDEVILLE. *J. Endodont.* (2002) to appear.
33. P. W. BROWN and M. T. FULMER, *J. Am. Ceram. Soc.* **74**(5) (1991) 934.
34. K. S. TENHUISEN and P. W. BROWN, *J. Mater. Sci. Mater. Med.* **7** (1996) 309 and refs 20–26 therein.
35. K. L. ELMORE and T. D. FARR, *Ind. Engr. Chem.* (1940) 580.

Received 19 February
and accepted 12 June 2002